

Rapidly-migrating and internally-generated knickpoints can control submarine channel evolution

Maarten S. Heijnen^{1,2,*}, Michael A. Clare¹, Matthieu J.B. Cartigny³, Peter J. Talling³, Sophie Hage², D. Gwyn Lintern⁴, Cooper Stacey⁴, Daniel R. Parsons⁵, Stephen M. Simmons⁵, Ye Chen⁵, Esther J. Sumner², Justin K. Dix², John E. Hughes Clarke⁶

¹Marine Geosciences, National Oceanography Centre, European Way, Southampton, U.K.

²Ocean and Earth Sciences, National Oceanography Centre, University of Southampton, European Way, Southampton, U.K.

³Departments of Geography and Earth Sciences, University of Durham, South Rd, Durham, U. K.

⁴Natural Resources Canada, Geological Survey of Canada, Box 6000, 9860 West Saanich Road, Sidney BC, Canada.

⁵School of Environmental Sciences, University of Hull, U.K.

⁶Earth Sciences, Center for Coastal & Ocean Mapping, University of New Hampshire, 24 Colovos Road, Durham, U.S.A.

*corresponding author: maarten.heijnen@noc.ac.uk

Abstract

Submarine channels are the primary conduits for terrestrial sediment, organic carbon, and pollutant transport to the deep sea. Submarine channels are far more difficult to monitor than rivers, and thus less well understood. Here we present the longest (9 year) time-lapse mapping yet for a submarine channel. Past studies suggested that gradual meander-bend migration, levee-deposition, or migration of (supercritical-flow) bedforms controls the evolution of submarine channels. We show for the first time how exceptionally rapid (100-450 m/year) upstream migration of 5-to-30 m high knickpoints can control how submarine channels evolve. Knickpoint migration changes the shape of the channel that exceeds change caused by progressive bend migration, and equals sediment volumes delivered to the submarine channel-head by the feeding rivers. Knickpoints in rivers are created by external factors, including tectonic movement, variability of substrate strength, or base-level change. However, the knickpoints in Bute Inlet cannot be linked to any of such external

32 factor. Similar knickpoints are common in submarine channels worldwide, and are thus of
33 global importance for how channels operate.

34 **Introduction**

35 Seafloor sediment flows called turbidity currents transport globally important
36 volumes of sediment, and form some of the deepest canyons, longest channels and largest
37 sediment accumulations on Earth¹⁻³. These and widespread underwater channel systems
38 can extend for tens to thousands of kilometres offshore, and their dimensions may rival or
39 even exceed those of terrestrial river systems^{4,5}. Turbidity currents that flush submarine
40 channels can be very powerful (reaching velocities of 20 m/s), and they pose a serious
41 hazard to seafloor infrastructure, which includes telecommunication cables that carry >95%
42 of global data traffic⁶⁻⁸. Furthermore, sediment, organic carbon, nutrients, and pollutants
43 that are transported via submarine channels, influence deep marine ecosystems and climate
44 on long time scales⁹⁻¹¹, while ancient channel deposits can form reservoirs and source rocks
45 for hydrocarbon production^{12,13}, and act as an archive for the Earth's history^{14,15}. There is
46 ongoing debate over terminology, but here we use 'submarine channel' to describe features
47 formed by net-erosion (i.e. canyons in some classifications), as well as by net-
48 deposition^{5,16,17}.

49 Despite the global occurrence and importance of submarine channel systems, there
50 are very few detailed time-lapse seabed surveys showing directly how channels change and
51 move through time. Channels can evolve over different timescales, ranging up to "channel
52 life cycles", encompassing channel inception, maintenance and abandonment, which can
53 span over geological times¹⁸. Here we describe how a submarine channel evolves during 9
54 years of its active (maintenance) stage, after initial formation and before final

55 abandonment. Understanding channel evolution, and what processes drive it, is important
56 to be able to understand how and where material is transported to by turbidity currents.
57 This can help to predict burial and re-excavation potential of organic carbon, nutrients and
58 pollutants, architecture of hydrocarbon reservoirs, as well as areas prone to geohazards.

59 We are aware of 13 locations where multiple bathymetric surveys of the modern
60 seafloor have provided time-lapse information on how active channels evolve
61 (Supplementary Table 1). These studies typically involve two surveys, cover periods of less
62 than five years, do not cover the full extent of a system from source to sink, or capture
63 relatively small delta-front systems. The highest resolution time-lapse study of a full-length
64 system is from the 1-2 km long delta-front channels on Squamish Delta, but this system is
65 being re-established after a man-made river diversion^{19,20}. This lack of time-lapse studies is
66 in stark contrast to the very large number of time-lapse studies of how river channels
67 evolve, which benefit from abundant airborne lidar, aerial photographs, and satellite
68 images²¹. There is a compelling need for detailed time-lapse studies to understand how
69 submarine channels evolve.

70 This lack of time-lapse data from full-length systems ensures that previous studies of
71 subaqueous channel evolution were mainly based on physical laboratory-scale modelling,
72 numerical models, geophysical (seismic) data, outcrop studies, comparisons to rivers, and
73 non-time-lapse seafloor mapping²²⁻²⁶. These studies have considerably advanced our
74 understanding of how submarine channels work. However, laboratory models suffer from
75 important scaling issues²³, and numerical models make assumptions that are often poorly
76 validated against full-scale field data. Seismic data and rock outcrops only capture the end
77 result of channel evolution, rather than a time series of how the channel evolved in
78 response to certain environmental conditions. Intervals dominated by erosion are especially

79 difficult to reconstruct using seismic data or rock outcrops. The resolution of seismic data is
80 often insufficient to resolve small features within channels. Rock outcrops also lack detailed
81 chronological data for quantifying rates of short-term processes, and may not give a full
82 three-dimensional perspective²⁷.

83 Despite these limitations, previous work has proposed three main processes that
84 might control the evolution of submarine channels. First, it has been proposed that
85 submarine channels evolve in a broadly comparable way to meandering rivers, via gradual
86 outer-bend erosion and inner-bend deposition, and meander bend cut-off^{5,25,28}. Gradual
87 meander-bend migration has long been known to be a dominant control on how rivers
88 evolve^{29,30}, but also occurs in submarine channels and is driven by secondary (across-
89 channel) helical flow^{12,31,32}. Meander-bend cut-off can result from bend-migration and affect
90 channel morphology, as commonly seen in rivers³³. However, submarine channels appear to
91 differ in key regards from rivers³⁴. There has been a vigorous debate over whether the sense
92 of secondary (across-channel) flow in turbidity currents is reversed with respect to
93 rivers^{27,31,35,36}. It has also been suggested that submarine channels tend to have fewer
94 meander-bed cut-offs than rivers³⁴, although, cut-offs are common in some submarine
95 channels^{28,37}. This debate also has led to modified models for submarine bend-growth and
96 their resulting sedimentary architecture⁵. Second, deposition of flanking levees may control
97 channel evolution by confining turbidity currents, by fixing the system in place and
98 regulating channel depth. This process has been proposed to be especially important in the
99 early stages of channel development. However, the exact role of levees in channel initiation
100 remains a topic of debate^{18,23,38,39}. Levee development may be especially important in highly
101 depositional channels, such as channels on the Amazon Fan and Bengal Fan^{1,40}. Third, it has
102 been suggested that turbidity currents have a greater tendency than rivers to be Froude-

103 supercritical (i.e. exist in a thin and fast state)⁴¹. Flow instabilities called cyclic-steps can
104 characterise these supercritical turbidity currents, causing repeated hydraulic jumps.
105 Crescent-shaped bedforms or repeated seabed scours, are common expressions of these
106 cyclic steps, which previous authors propose play a key role in submarine channel evolution
107 and deposit geometries^{19,24,42–46}. Trains of seafloor scours, attributed to cyclic steps, have
108 also been proposed to initiate channels^{18,42}.

109 Here we test these models and propose a fourth possible major control on
110 submarine channel evolution; internally-generated and rapidly-migrating knickpoints.
111 Knickpoints are steep steps in channel gradient that migrate upstream via erosion^{47,48}, and
112 they are common in river systems^{49–51}. Fluvial knickpoints typically result from external
113 controls such as base-level change, resistant bedrock layers, or tectonic movement⁴⁸. The
114 knickpoint's steep face enhances the erosive potential of flow, causing the knickpoint to
115 migrate upstream. Sediment flux downstream of the knickpoint increases as a result of this
116 enhanced erosion, causing more deposition on the next lower gradient section
117 downstream⁵². Knickpoints in rivers typically migrate at rates of 0.001 m/yr to 1 m/yr,
118 depending mainly on discharge and rock strength, but can sometimes reach 1000 m/yr due
119 to flash-floods or weak substrate^{49–51}. Previous studies have described knickpoints in
120 submarine (and sublacustrine) channels in various settings worldwide (Supplementary table
121 2). Initiation of these knickpoints has also been attributed to external controls such as
122 bedrock or tectonics, meander-bend cut-off, or to cyclic step instabilities within supercritical
123 turbidity currents^{22,53–56}.

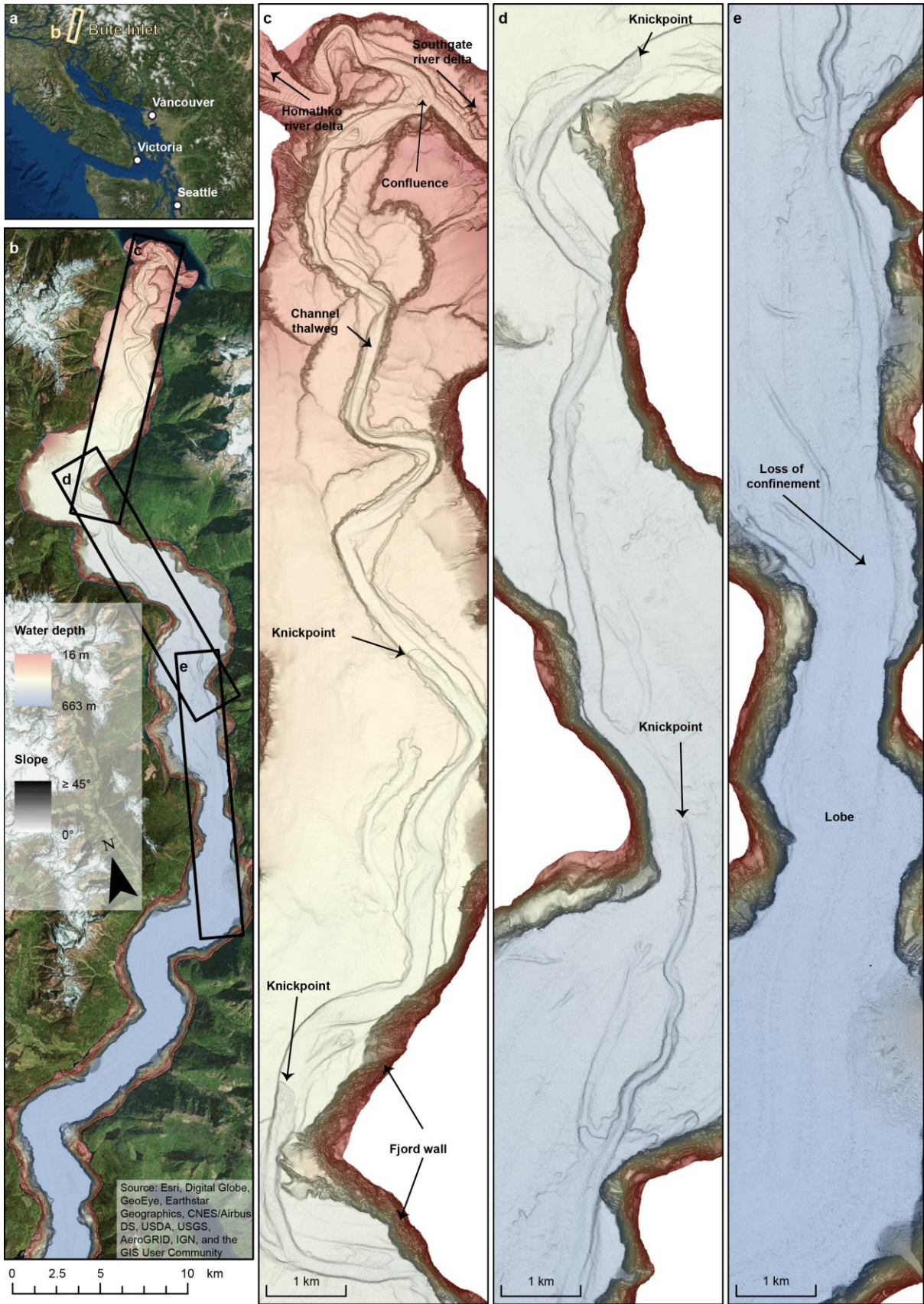
124 **Aims**

125 Here we present the most detailed time-lapse mapping yet for an active submarine
126 channel, over its full length of ~40 km, to understand the role of migrating knickpoints in
127 submarine channel evolution. These data comprise 5 bathymetric surveys over 9 years
128 (2008-2016) in Bute Inlet, British Columbia, Canada (Fig. 1). These data allow us to
129 document how a submarine channel evolves along its full length, for almost a decade.

130 Our initial aim is to understand what factors can control the evolution of submarine
131 channels. These time-lapse surveys show that the evolution of this submarine channel is
132 dominated by exceptionally rapidly migrating knickpoints. Our second aim is therefore to
133 understand what causes these very fast-moving knickpoints. Our third aim is to understand
134 the implications of these rapidly-migrating knickpoints for submarine channel-bend
135 evolution, and deposits preserved within channels. We provide new generalised models for
136 both bend evolution and channel deposits. We conclude by showing that similar submarine
137 knickpoints occur in many locations, and may thus have widespread importance for how
138 submarine channels work, and how their deposits form.

139 **Geographical setting**

140 Bute Inlet is located in British Columbia, West Canada (Fig. 1a). The head of this fjord is fed
141 by the Homathko River and Southgate River, responsible for respectively 80% and 15% of
142 the freshwater input in the system (remaining 5% from smaller rivers coming from the side
143 of the fjord)⁵⁷. The rivers are mainly fed by glacial meltwater, with much higher discharges
144 in summer. Homathko River has an average summer discharge of 600 m³/s, with maxima
145 above 1000 m³/s, while winter discharges are typically below 100m³/s. It has been
146 estimated that these rivers supply ~1.6 million m³ of sediment to the fjord each year⁵⁷. A
147 ~40 km long submarine channel is present on the floor of Bute Inlet, and it originates at the



148

149

150

Figure 1: Overview of the submarine channel system in Bute Inlet. a) Location of Bute Inlet in British Columbia, Canada. b) Map of Bute Inlet showing the location of more details images shown in panels

151 *c to e. Bathymetric surveys are presented here as maps of seabed gradient, which optimally visualise*
152 *small and steep topographical features, such as knickpoints. Seabed gradient maps are then overlain*
153 *by a transparent bathymetry map. c-e) Detailed maps of the 40 km long submarine channel within*
154 *Bute Inlet, showing the location of river deltas, knickpoints and lobe beyond the channel mouth.*

155 pro-deltas of the two main rivers^{58,59}. The channel is 35 m deep in the most upstream part
156 of the system, and its depth decreases gradually downstream towards the depositional area
157 (terminal lobe), beyond the channel termination at 620 m water depth⁶⁰ (Supplementary
158 Fig. 1).

159 The floor of the channel comprises sand, whilst the surrounding fjord is dominated
160 by mud^{58,60}. Turbidity currents occur frequently along the upper channel, with over 10 flows
161 a year, which occur coincident with periods of higher river discharge in the spring and
162 summer^{59–61}. More recent and higher resolution bathymetric surveys demonstrated that the
163 submarine channel in the Bute Inlet system is strongly altered by these turbidity currents,
164 with 25% of the channel having changed by 5 metres or more within three years⁶² and
165 showed active upstream migrating knickpoints⁶³. Here we analyse a longer time series over
166 a more extensive area of the submarine channel in Bute Inlet.

167 **Results**

168 A difference map captures bathymetric changes in the channel for the entire study
169 period between March 2008 and October 2016 (Fig. 2a). It covers the full length of the
170 channel, and the area immediately beyond the channel termination (terminal lobe). The
171 channel floor is characterised by alternating areas of erosion and deposition (Fig. 2a), a
172 pattern that is repeated three times along the channel (Fig. 2a; 3a). The three main
173 erosional areas are bounded at their upstream sides by a steep (up to ~30°) face that is 5–30

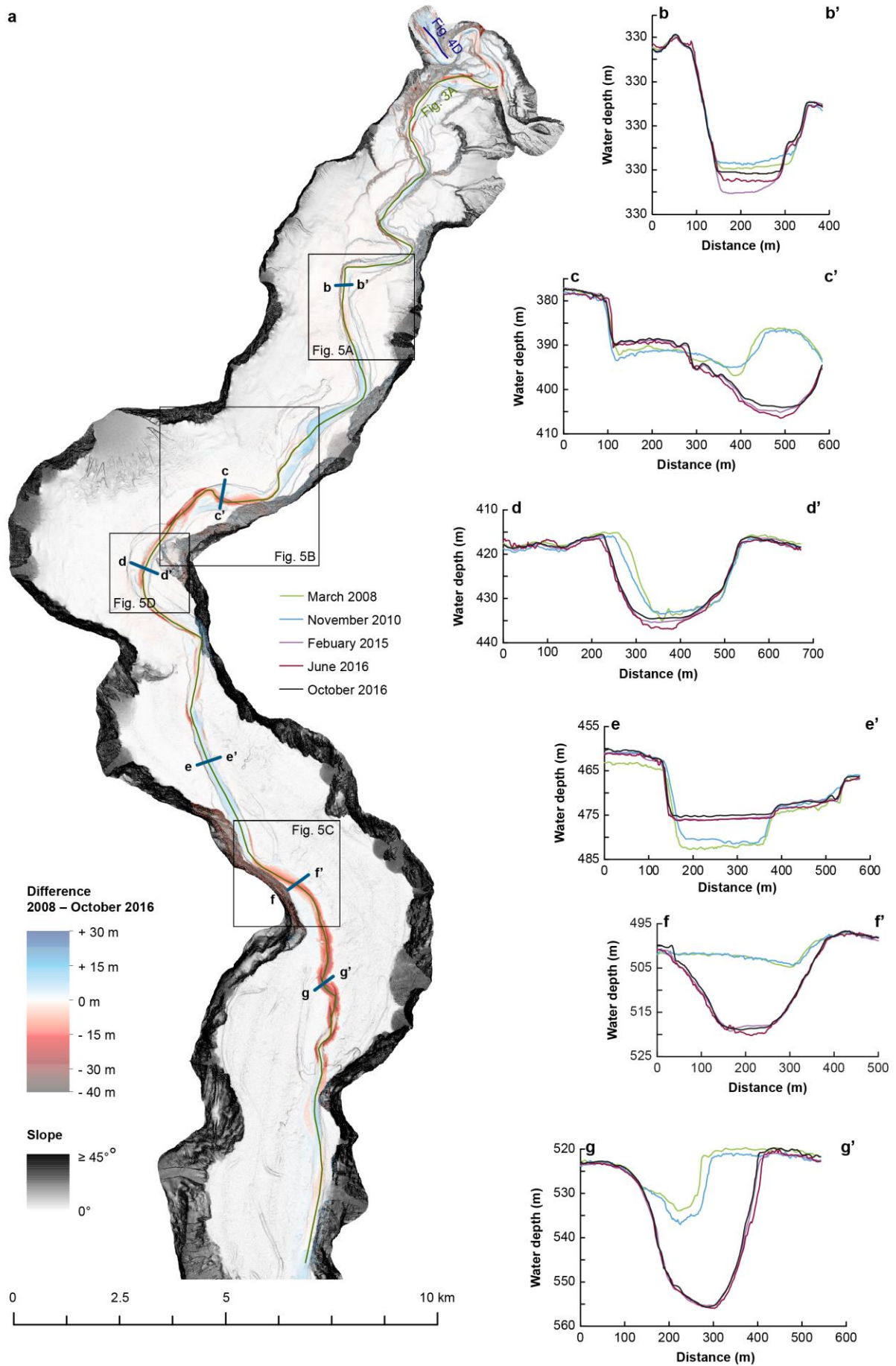
174 m high. Similar steep steps are found within each erosional area. We call these steep steps
175 'knickpoints', and we refer to erosional areas that consist of several knickpoints as a
176 'knickpoint-zones'. Knickpoints bounding the knickpoint-zone at its upstream side are
177 termed 'frontal-knickpoints'. Repeat surveys show that frontal-knickpoints and associate
178 knickpoint-zones migrate upstream between each pair of surveys (Fig. 2a; 3a,b; 4a-c).

179 We also observe crescent shaped bedforms in the channel. We differentiate
180 between these bedforms and knickpoints based on scale and shape. The crescent shaped
181 bedforms are smaller (1-5 m high), and have a more consistent wavelength (50-100 m) than
182 the knickpoints. The bedforms have a rounded crest, and an upstream-dipping stoss side.
183 Crescent shaped bedforms can be superimposed on knickpoints. The knickpoints themselves
184 are 5-30 m high, are spaced 1–3 km apart in knickpoint zones, and have a sharp crest.

185 The pattern of alternating zones of erosion and deposition is lost in the furthest
186 upstream part of the system, above 300 m water depth (Fig. 3). The knickpoints and the
187 erosion in the knickpoint zones progressively decrease in size upstream. Very small
188 knickpoints might occur in this upstream part of the system, but it becomes difficult to
189 distinguish them from crescent shaped bedforms. To understand the role of knickpoints in
190 channel evolution, we therefore focus on the well-defined knickpoints in the main three
191 knickpoint-zones.

192 Knickpoint-zone 1

193 We now describe each of the three main knickpoint-zones, which are numbered from 1 to 3
194 in a down-channel direction (Fig. 3). Knickpoint-zone 1 migrates through a pre-existing
195 channel bend during the time covered by the surveys. The knickpoints are focussed towards
196 the outside of the bend (Fig. 5a). The knickpoint-zone consisted of a single frontal-

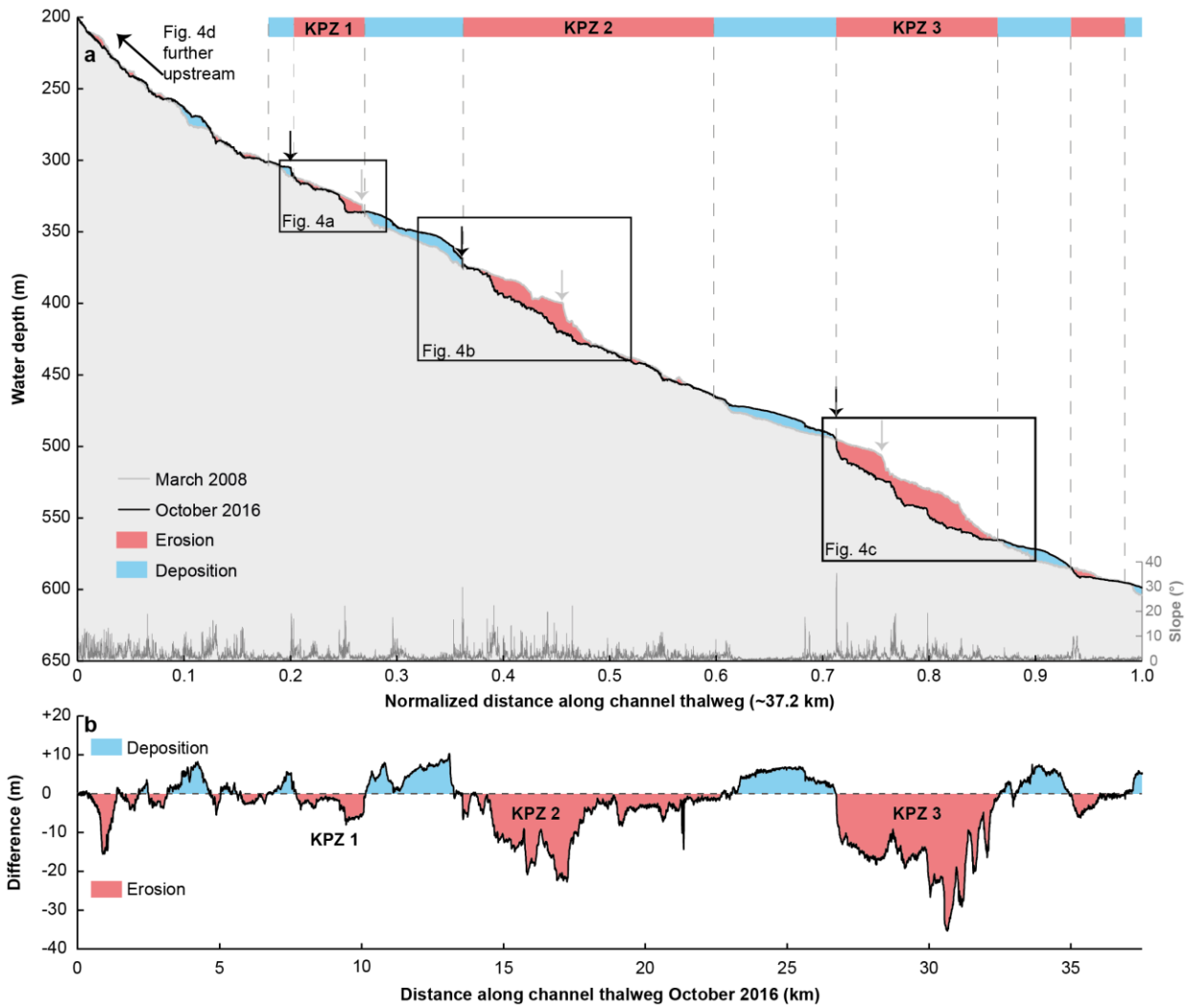


198 *Figure 2: Changes in the submarine channel in Bute Inlet. a) Map of changes in seabed elevation*
199 *between March 2008 and October 2016 shown by a red-to-blue colour-scale, overlaying a seabed*
200 *gradient in grey-scale. Note the alternations of deposition and erosion along the channel. b-g)*
201 *Changes in seabed elevation at a series of cross-sections, locations are shown in panel a. Vertical*
202 *exaggeration: 10. b) Channel gradually fills until knickpoint zone arrives in October 2016, and incises*
203 *into previous deposits. c) Lateral migration of channel thalweg as a result of knickpoint migration.*
204 *Note how the channel floor in 2008-2010 becomes a terrace from 2015 onwards. d) Section showing*
205 *largest observed amount of outer-bend erosion away from migrating knickpoints. e) Progressive*
206 *filling of a channel in a depositional area. f) Knickpoint migration creates a channel, where the*
207 *channel was previously shallow and poorly-defined. g) Cross section at location affected by both*
208 *outer-bend erosion and knickpoint migration.*

209 knickpoint that was ~20 m high in March 2008 (Fig. 4a; 5a). A second knickpoint developed
210 in the knickpoint-zone by February 2015 (Fig. 4a; 5a). Both knickpoints are about 10 m high
211 from February 2015 onwards. The frontal-knickpoint migrated ~2.5 km upstream between
212 March 2008 and October 2016, averaging at 280 m/yr. The knickpoint migration has caused
213 up to 20 m of channel floor erosion.

214 Knickpoint-zone 2

215 Knickpoint-zone 2 is located downstream of a relatively wide segment of the channel
216 (Fig 5b). The frontal-knickpoint was 25 m high in March 2008 and November 2010, and
217 migrated at the outer side of a pre-existing channel bend. After 2010, migration of the
218 knickpoint-zone completely reshaped the channel morphology, creating a new narrower
219 and more sinuous channel. The thalweg in one of the new bends migrated partly outside the
220 original channel (Fig. 2b; 5b). Part of the original channel turned into a terrace after
221 knickpoint migration. The frontal-knickpoint is much smaller (~15 m) and less active after



222

223

224

225

226

227

228

229

230

231

232

Figure 3: Change along channel profiles, and resulting patterns of erosion and deposition, from March 2008 to October 2016. Location is shown in Fig. 2a. KPZ = Knickpoint-zone a) Bathymetric profiles along the channel thalweg in 2008 and October 2016. Vertical exaggeration: 50. The position of the channel shifts as the channel evolves, so profiles were constructed along the position of the thalweg in that survey. Profiles were then normalised to allow comparison. Slope was generated using the survey from October 2016. Note the downstream alternation of deposition (blue) and erosion (red). Three main erosional areas (knickpoint-zones) are bounded at their upstream end by steep steps (frontal-knickpoint) in the channel profile. Additional smaller knickpoints are often present within wider knickpoint-zones. Proximal erosion upstream of knickpoint-zone 1, is due to lateral migration of the channel, unrelated to knickpoint migration. b) Difference in channel

233 *elevations between March 2008 and October 2016 along the channel thalweg. Migration of three*
234 *knickpoint zones (KPZ 1 to 3) produces erosional areas (in red).*

235 February 2015. The average rate of frontal-knickpoint migration was ~300 m/yr over the
236 entire survey, with the fastest rates of ~440 m/yr occurring between 2010 and 2015.

237 Knickpoint-zone 3

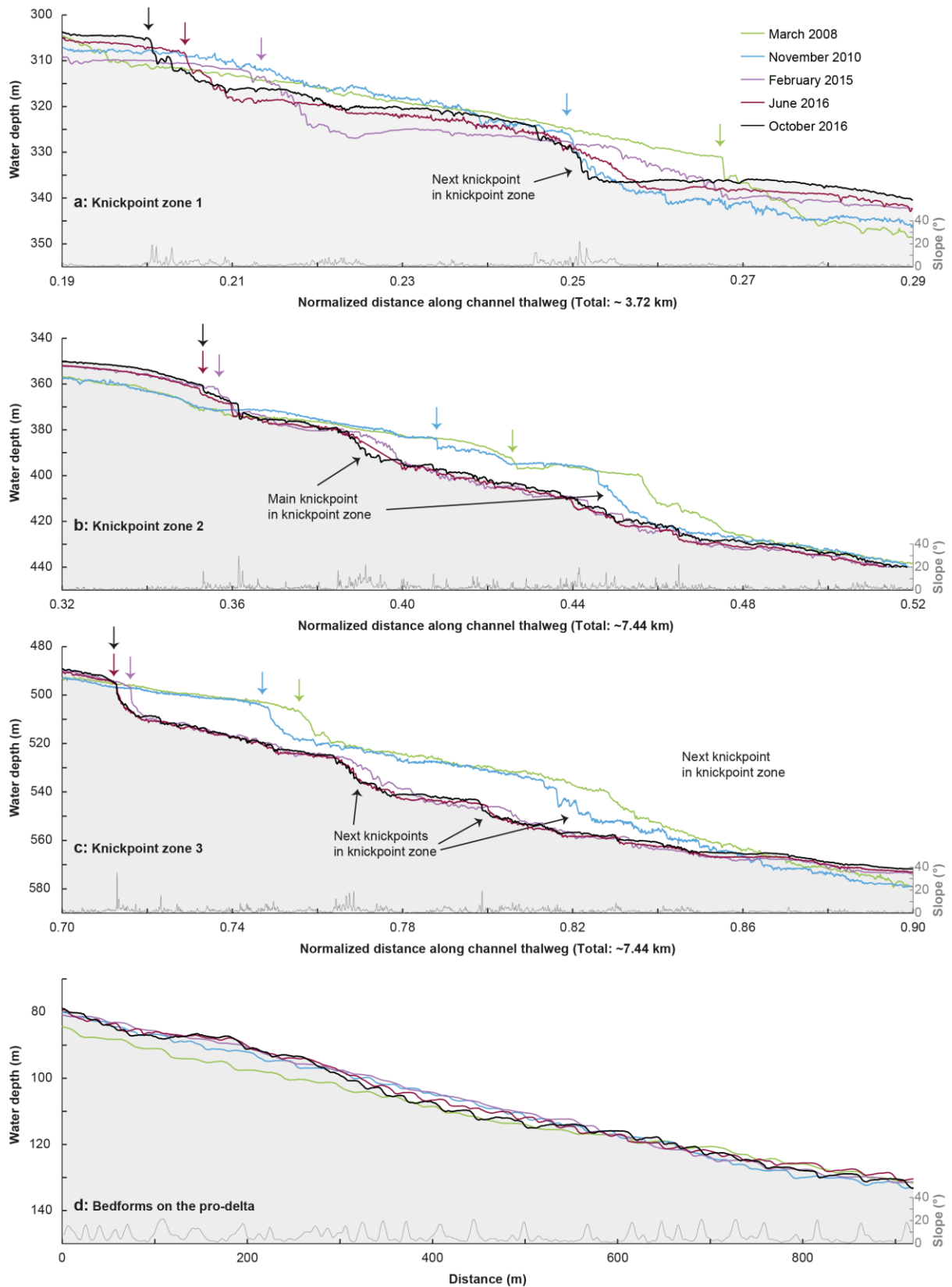
238 Knickpoint-zone 3 lies downstream of an area where the channel is not well
239 developed (Fig. 2e; 5c). The height (~15 m) of the frontal-knickpoint remains near-constant
240 through the study period. Migration of the frontal-knickpoint involved erosion into
241 previously deposited (before 2008) sediments, creating a ~20 m deep and well-defined
242 channel in locations where the channel was previously much shallower (10 m). The frontal-
243 knickpoint migrated ~1.8 km upstream during the 2008-2016 period, at a rate of ~200 m/yr.
244 A second large (~30 m), but less-steep knickpoint can be recognised in 2008 and 2010,
245 whilst two smaller (~15 m high) knickpoints follow the frontal-knickpoint from 2015
246 onwards.

247 Rates of knickpoint migration

248 These time-lapse surveys show that individual knickpoint-zones typically migrate at
249 rates of several hundreds of meters a year. The fastest documented migration rate was 440
250 m/yr. These migration rates are thus 2-to-6 orders of magnitude faster than most
251 knickpoints in rivers, which commonly migrate at rates of only 0.001 m/yr to 1 m/yr⁴⁹.

252 Outer-bend erosion

253 Outer-bend erosion resulting in lateral migration of the channel is common in Bute
254 Inlet, causing channels to migrate laterally up to 120 m over the entire length of the survey



255

256

257

258

Figure 4: Temporal changes in submarine channel profiles. a-c) Detailed time-lapse changes in profiles across knickpoint-zones 1, 2 and 3, whose locations are indicated in Fig. 3a. Vertical Exaggeration: 20. Slope was generated using the survey from October 2016. Arrows indicate the

259 *position of the frontal frontal-knickpoint in each survey. d) Profile along the shallow-water pro-delta*
260 *channel, as indicated in Fig. 2a, where crescentic shape bedforms dominate and no knickpoints are*
261 *present. Vertical exaggeration: 5. Note the relatively small amount of bathymetric change, when*
262 *compared to the three knickpoint zones.*

263 (Fig. 2a,c,d,g 5d). While some progressive outer-bend erosion is observed in locations
264 unaffected by knickpoint migration (Fig. 2d), outer-bend erosion is enhanced strongly where
265 it is coincident with knickpoint migration (Fig. 2f).

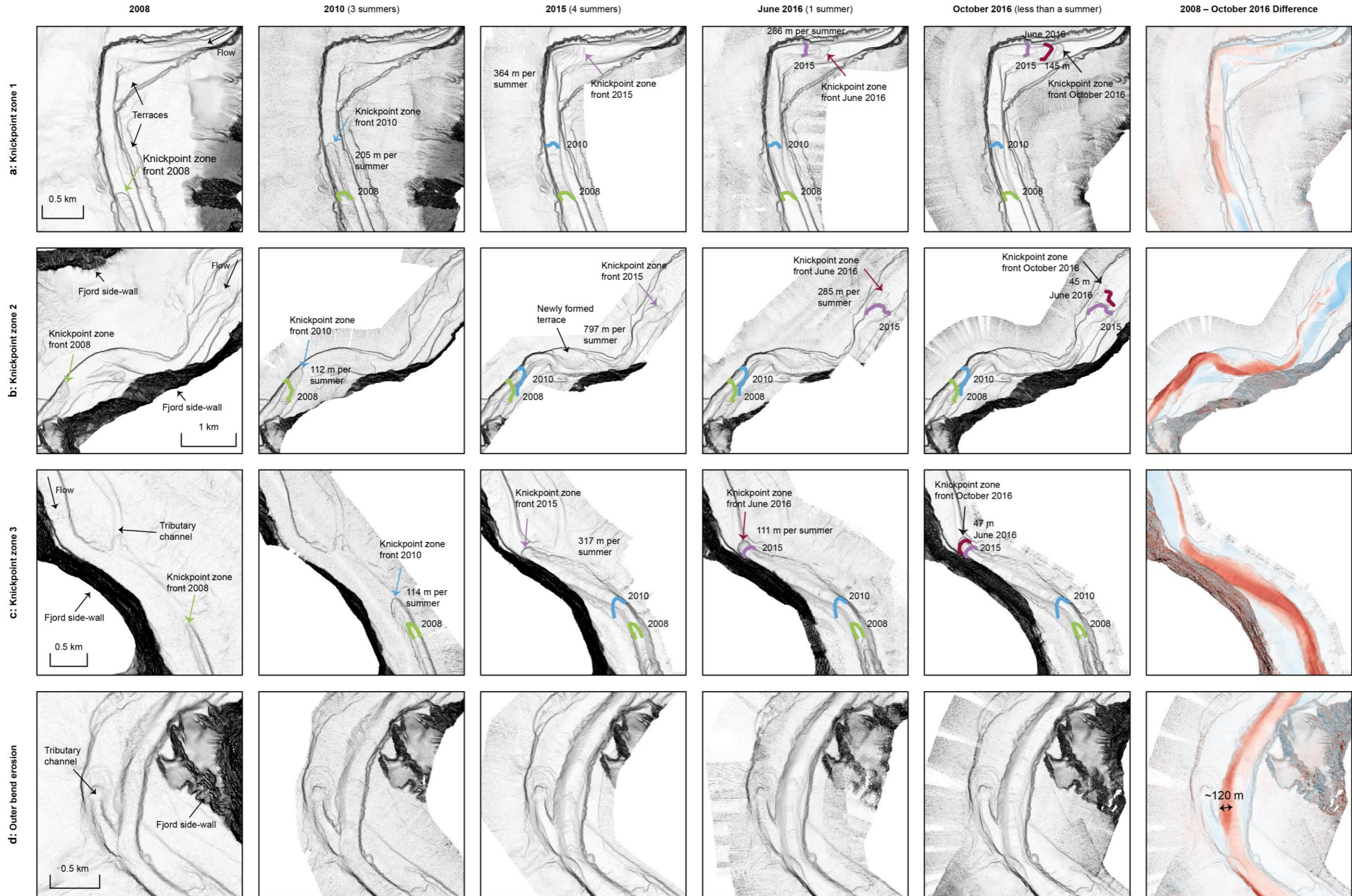
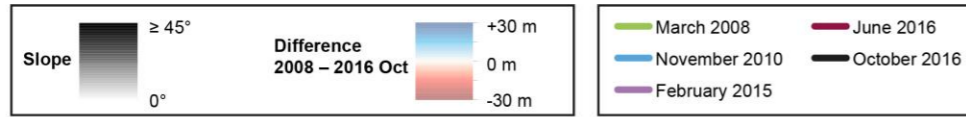
266 Crescentic shaped bedforms

267 Crescent shaped bedforms are easily resolvable in the deeper part of the system,
268 due to the vertical resolution of the multibeam surveys. The prodeltas are dominated by
269 crescent shaped bedforms, and do not experience knickpoint migration. Changes in seabed
270 elevation (< ~10 m) associated with crescentic bedform migration here are much less than
271 changes (of up to 25 m) associated with knickpoint migration (Fig. 4d).

272 Levee development

273 Levees are a distinct feature in many submarine channels where levee crests may rise over
274 100 m above the surrounding seafloor^{1,40}. The levees in Bute Inlet are maximum 10 m, but
275 typically less than 5 m high (Supplementary Fig. 2e,f). Channels here have a negative relief
276 compared to the surrounding floor of the fjord, rather than bound by levees and rising
277 above the surrounding seafloor. No significant levee aggradation is recorded during the time
278 of the survey.

279



281 *Figure 5: Time-lapse maps showing areas of channel evolution in detail, locations are indicated in Fig.*
282 *2a. Migration rate of the frontal-knickpoint is indicated in each panel. a) Evolution of knickpoint-zone*
283 *1. b) Evolution of knickpoint-zone 2. Knickpoint migration creates a narrower and more sinuous*
284 *channel. c) Evolution of knickpoint-zone 3. Knickpoint migration creates a channel, where previously*
285 *no well-developed channel existed. d) Erosion of an outer-bed. This is the greatest amount of outer-*
286 *bend erosion away from migrating knickpoints, seen in the Bute Inlet channel. The amount of change*
287 *is less than that associated with knickpoints 1-3.*

288 Eroded volumes

289 Difference maps were used to calculate volumes of sediment eroded. We compared
290 the total erosion in the channel, erosion caused by knickpoint migration, and outer-bend
291 eroded sediment independent from knickpoint migration. The total amount of erosion in 9
292 years over the entire length of the active channel is $39 \times 10^6 \text{ m}^3$. Of that total eroded
293 volume, $28 \times 10^6 \text{ m}^3$ can be attributed to knickpoint migration, which is 72% of total eroded
294 volume, and similar to the amount of sediment transported into the system. Outer-bend
295 erosion accounts only for $8 \times 10^6 \text{ m}^3$ (21%) of the total eroded volume, which is about 30%
296 of the amount of sediment delivered to the system (Supplementary Fig. 3).

297 **Discussion**

298 Testing previous models for channel evolution

299 Our first aim is to understand what controls submarine channel evolution. It has
300 previously been suggested that secondary (across-channel) helical flow causing gradual
301 bend migration, is the main control on submarine channel evolution, as is the case for many
302 rivers. There has been considerable debate over whether the sense of submarine secondary
303 circulation is river-like or reversed^{27,31,35,36}. Outer-bend erosion causing lateral migration is

304 common in Bute Inlet and can locally reach rates of over 10 m/yr. This is fast, even
305 compared to rapidly migrating meandering rivers³², and almost an order of magnitude
306 higher than the incision rate. However, our study shows that outer-bend migration can be
307 linked to knickpoint migration (Fig 2g), rather than gradually, as observed in rivers. This
308 knickpoint-related lateral migration offers a possible mechanism explaining the punctuated
309 migration inferred from submarine channel deposits⁶⁴. However, we do not observe major
310 sediment deposition at inner-bends. Furthermore, long stretches of the channel in Bute
311 Inlet are straight (around Fig. 2e), and not characterized by expanding meander bends, like
312 some other systems are^{28,37}. Secondary flow therefore does not always play the key role in
313 channel evolution, irrespective of the sense of that secondary flow compared to rivers.

314 Pervasive crescent-shaped bedforms on the delta-front are most likely a record of
315 cyclic steps in supercritical turbidity currents, as similar-scale bedforms have been linked to
316 cyclic steps in supercritical flows at nearby Squamish Delta^{19,46}. These bedforms can be an
317 important control on submarine channel evolution in other systems^{20,45}. However, we show
318 that knickpoints play a more dominant role in Bute Inlet channels. We later discuss whether
319 the knickpoints themselves are a supercritical flow bedform, albeit at a larger scale.

320 Meander bend cut-offs can be very common in other systems^{28,37}. It appears that
321 meander bend cut-offs are not a major control on channel evolution in Bute Inlet, as none
322 are observed in our surveys, nor are any signs of previous cut-offs observed. Finally,
323 previous work has suggested that deposition of levees plays a key role in flow-confinement,
324 and thus channel evolution^{23,65,66}. This process is hypothesised to be especially important on
325 longer timescales, since we do not see significant deposition on the levees. However, we do
326 see new confinement being formed independent of levees through the migration of

327 knickpoints. These knickpoints can create a well-developed channel where no clear channel
328 existed previously (Fig. 5c). Similar processes have been shown in flume tank experiments
329 where new channels were initiated by upstream-migrating erosional features^{67,68}. However,
330 such fast-moving knickpoints were never monitored in this detail previously at field scale.
331 Furthermore, the channel in Bute Inlet confines flows by being incised in the seafloor rather
332 than through deposition of levees rising above the seafloor.

333 Exceptionally fast-moving knickpoints can dominate submarine channel evolution

334 Here we show for the first time that fast-moving knickpoints can dominate the
335 evolution of a submarine channel. Upstream-migrating knickpoints in Bute Inlet are
336 exceptionally fast-moving (100-450 m/year. This is 2-6 orders of magnitude faster than
337 typical knickpoint migration rates in rivers, which are 0.001 m/yr to 1 m/yr⁴⁹. Migration
338 rate of knickpoints has only been documented in two subaqueous channels^{69,70}, where they
339 move upslope at rates of 50–200 m/yr, comparable to those seen in Bute Inlet. These
340 studies did not focus on the knickpoints and their role in submarine channel evolution.
341 Flume tank experiments of knickpoints previously suggested fast (0.5 mm/s) migration rates
342 of knickpoints⁶⁸, and are supported by these data. However direct comparison of erosion
343 rates between experiments and natural systems remains difficult, due to scaling issues
344 inherent in experiments. The migration rate of these knickpoints is also very high
345 compared to other big bedforms, such as tidal bars and aeolian dunes, that migrate up to
346 10s of meters per year^{71,72}. Submarine knickpoints can also cause lateral migration of a
347 channel thalweg (Fig. 5b), or incise new channel sections channels in places where no well-
348 defined channel was previously present (Fig. 5c).

349 Rapid sediment deposition occurs in channel reaches between knickpoint-zones.
350 These deposits most likely represent downstream accumulation of sediment eroded by the
351 upstream knickpoint, as can occur in rivers⁵². However, the volume of sediment deposited
352 downstream of the knickpoints appears to be smaller than eroded volume upstream (Fig.
353 2a, 3). This difference could be due to part of the initially eroded knickpoint sediment being
354 transported further downstream, and deposited on the distal lobe.

355 Volumetric estimates of surface change also demonstrate the dominance of
356 knickpoints. Within the channel, the volume of sediment erosion by upstream-migrating
357 knickpoints accounts for ~72% of the total observed erosion, equalling the volume of
358 sediment supplied by the main river at the top of the channel during the same period. Even
359 though erosion related to knickpoint migration appears to exceed the deposition during the
360 survey period, knickpoints migrated during erosion into recently deposited channel-filling
361 sediments (Fig. 2b; 4a). This re-incision into recent deposits can explain why migration of
362 many individual 5-30 m deep knickpoints, over periods of centuries to millennia, has not
363 carved a channel deeper than ~30m along this fjord. Phases of erosion caused by upstream-
364 migrating knickpoints, followed by phases of deposition, appear to create a balance such
365 that the channel depth is approximately that of a single knickpoint (5-30 m).

366 Reworking of recently deposited, and thus poorly consolidated sediment could partly
367 explain why knickpoint migration is so rapid. Fresh channel deposits are mostly sand-
368 dominated^{58,60}, and they may be prone to erosion and failure, especially when loaded or
369 scoured by fast moving turbidity currents. This kind of substrate may be much weaker than
370 older, and far more consolidated or strongly cemented sediments or bedrock that underlies
371 many river systems.

372

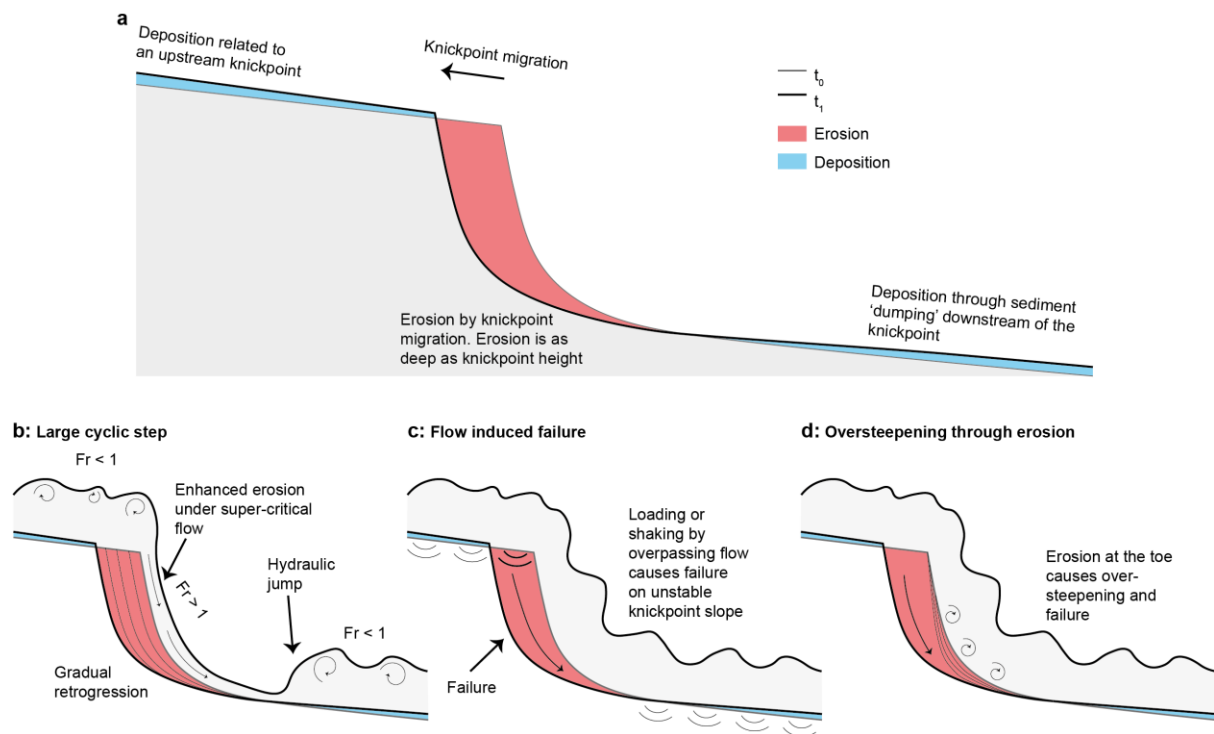
373 How do knickpoints migrate?

374 Knickpoints migrate upstream along the channel, and sometimes tend to migrate
375 towards the outer bend (Fig. 5 a,b), so they migrate to where flows are coming from. We
376 therefore interpret that their migration is caused by turbidity currents common in Bute
377 Inlet⁵⁹⁻⁶¹.

378 We propose three internal flow-substrate processes that could trigger knickpoint
379 migration, either in isolation or in combination (Fig. 6). The first model is that submarine
380 knickpoints, and intervening areas of deposition, are a large-scale bedform produced and
381 maintained by instabilities within supercritical flow^{42,54,73,74}, but with far longer wavelengths
382 (> 1-5 km) than those of the crescentic bedforms (typically 50-100 m in Bute Inlet; Fig 4d).
383 The second model is that migrating knickpoints are formed by seabed failures triggered by
384 rapid undrained loading of the substrate, as a turbidity current passes. Unusually rapid rates
385 of sediment accumulation (up to 1 m/year) in the depositional areas of the channel floor
386 may favour such failure^{75,76}. Past work suggested this model to explain the migration of sub-
387 lacustrine knickpoints in tailing deposits⁷⁷. These studies show that failure and subsequent
388 knickpoint migration can even occur unrelated to an overpassing turbidity current. Third,
389 the base of knickpoints may be gradually eroded and undercut by turbidity currents, leading
390 to oversteepening and failure²². This process is similar to headwall undercutting described in
391 waterfalls and is known to cause migration of knickpoints in rivers, albeit at much slower
392 rates^{50,78}.

393 We conclude that all three model are potentially consistent with available field data.
394 It is thus uncertain which model is correct, and more detailed monitoring will be needed to
395 discriminate between competing hypotheses with confidence.

396



397

398 *Figure 6: Contrasting models for knickpoint migration. a) Generalised pattern of erosion and*
 399 *deposition associated with upstream-migration of knickpoints. b) Cyclic step model. Knickpoint is*
 400 *formed by repeated instabilities (termed cyclic steps) that are self-generated by supercritical turbidity*
 401 *currents, which lead to hydraulic jumps. c) Flow-induced slope-failure model. Knickpoint results from*
 402 *sudden failure of the channel floor, when loaded during passage of a turbidity current. d)*
 403 *Oversteepening through erosion model in which erosion at the toe of the steep face causes*
 404 *oversteepening, and eventual failure.*

405 How are submarine knickpoints created or destroyed?

406 These three models (Fig. 6) explain the movement of existing knickpoints, rather
 407 than their initial origin or final disappearance. We consistently observe three knickpoint-
 408 zones in our time-lapse surveys (Fig. 3; 4a-c). Some additional small knickpoints appear
 409 within these zones, but they may be due to break-up of a larger knickpoint (Fig. 4a-c). Thus,
 410 we do not record clear examples of when a new knickpoint-zone formed, though we can
 411 speculate on their creation.

412 Knickpoints are common in river systems, where they are related to external factors.
413 Such external factors include local tectonic movement, variability in substrate or bedrock
414 strength, or base-level change⁴⁸. However, in Bute Inlet none of the knickpoints can be
415 related to any of these external factors. There is no evidence of local active tectonics, based
416 on seismographs that locate earthquakes. The submarine knickpoints are carved mainly into
417 recently-deposited channel-fill sediment^{58,60} (Fig. 2a; 4a), making a strong bedrock or
418 substrate control unlikely. As the channel is underwater, changes in sea-level (base-level)
419 will not produce knickpoints. Furthermore, these submarine knickpoints are not created by
420 meander-bend cut-offs, as observed in rivers, and modelled for submarine channels⁵⁶.
421 There are no meander bend cut-offs or remnants of meander bend cut-offs along the Bute
422 Inlet submarine channel (Fig. 1; 2a).

423 The lowermost knickpoint in knickpoint-zone 3 was in 2008 only 5-10 km away from
424 the channel to lobe transition zone (where channel confinement ends and sediment
425 deposits in a lobe⁷⁹). Assuming a constant migration rate of 200 m/yr in knickpoint-zone 3,
426 would suggest this knickpoint was at the channel-to-lobe transition zone around 1958–
427 1983. We would expect to see signs of some such external controls, if those created
428 knickpoints in the recent past. Therefore, it appears that knickpoints can be created in
429 submarine systems internally. If we rule out that knickpoints are created far beyond the
430 downstream end of the system, we suggested that knickpoints are created by internal
431 dynamics around the channel-to-lobe transition zone. A small steep step in channel gradient
432 can be observed around this area, which may eventually form the next knickpoint-zone (Fig.
433 3a).

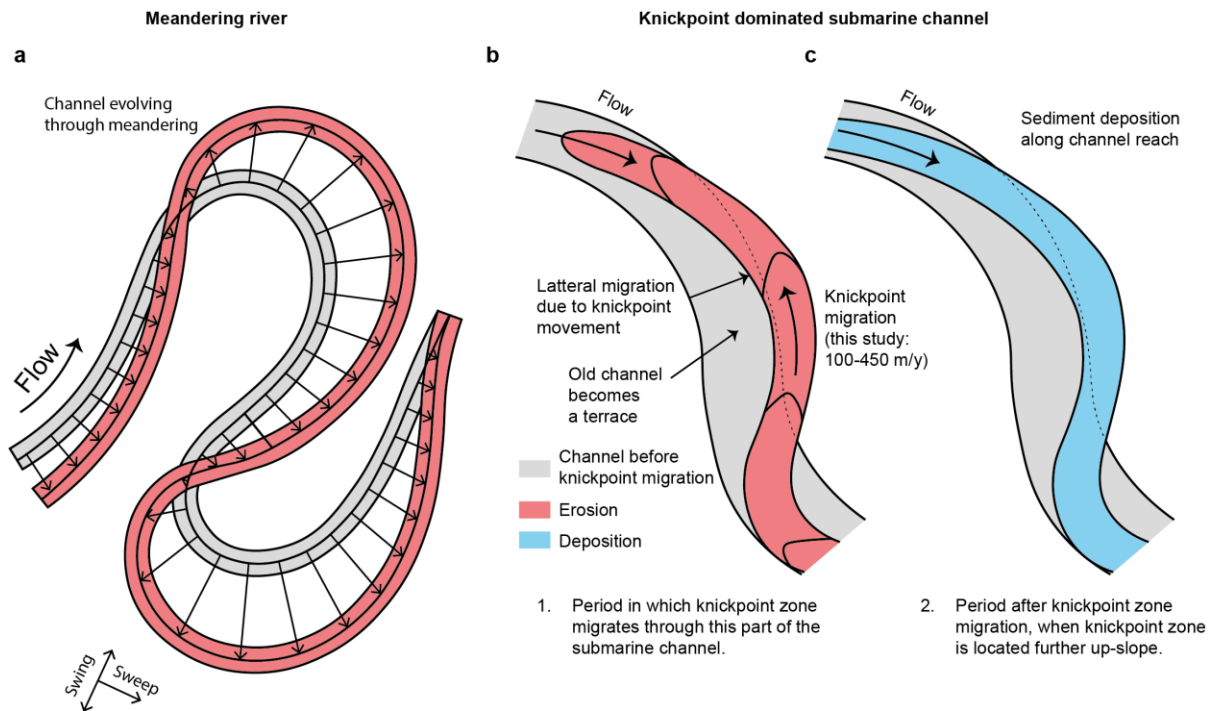
434 The exact origin of these knickpoint zones thus remains unclear at present. Similarly,
435 we do not see the disappearance of knickpoint zones as they migrate up-channel over the

436 nine years of our surveys. Further observations are thus also needed to establish how
437 knickpoints are born and disappear, potentially through even longer-term repeat surveys.

438 Implications for evolution of submarine channel-bends

439 We now seek to understand how knickpoint migration affects the evolution of
440 submarine channel bends. The planform evolution of meandering river bends is dominated
441 by secondary (across-channel) helical flow, which causes point-bar deposition on the inner-
442 bend, and erosion of the outer-bend²⁹ (Fig. 7a). This in turn causes river meander bends to
443 progressively increase in amplitude (swing) and translate downstream (sweep)^{32,80,81} (Fig.
444 7a). Recent work has shown how secondary flow patterns in submarine turbidity currents
445 may differ from that of rivers^{27,31,35,36}. A recent review found that submarine channel bends
446 evolve in different ways depending on what kind of bend-related (often bank attached) bars
447 form⁵. These bars are controlled by patterns of near-bed secondary flow, or direct
448 suspended load fallout. This would result in submarine channel evolution being driven by
449 deposition in bend-related (often bank-attached) bar deposits.

450 However, here we observe that submarine channel-bend evolution is dominated by
451 extremely rapid knickpoint migration, causing sudden channel-wide erosion (Fig. 2 and 3).
452 Rapid sediment deposition then occurs in channel-reaches downstream from knickpoint-
453 zones (Fig. 2a,e), rather than formation of distinct bend-related bars. Our surveys also show
454 that migration of knickpoints can extend outside the original channel, and thus create
455 terraces (Fig. 5b). This, combined with the lack of meander bend cut-offs or gradually
456 migrating bends, produces a rather different view of evolution of channel-bends than
457 previously described^{5,25} (Fig. 7b).



458

459 *Figure 7. Comparison between migration of channel bends in meandering rivers (after Sylvester et al.,*
 460 *2019), and submarine channels dominated by fast-moving knickpoint zones (this study). (a) Outer-*
 461 *bank erosion leads to swing and sweep of bends in a meandering river. (b) Rapid knickpoint zone*
 462 *migration in a submarine channel leads to lateral migration and terrace formation. (c) Knickpoint*
 463 *zone migrates further up-slope, and this part of the submarine channel is then infilled by deposition.*
 464 *Deposited sediment is partly sourced from knickpoint erosion located further up-slope.*

465 Implications for submarine channel deposits

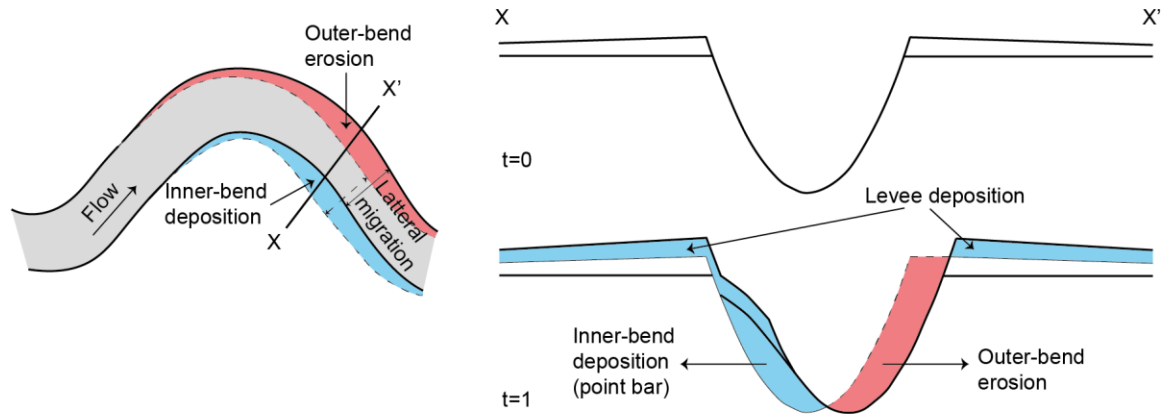
466 Knickpoint migration can also have a profound impact on the detailed architecture of
 467 channel-fill deposits (Fig. 8). Knickpoint migration is mainly associated with erosion into and
 468 reworking of previous sandy deposits within the channel-fill (Fig. 2b). Sediment is deposited
 469 gradually (~1 m/yr) downstream of kinckpoints and channel-wide sheets extending several
 470 kilometres downstream (Fig. 2a,b; 8b). These patterns of deposition and erosion due to
 471 knickpoints are fundamentally different to the bend-related bars predicted previously,
 472 based on more gradual bend-migration driven by secondary across-channel flow^{5,25} (Fig. 8a).

473 Submarine channels can be subdivided according to whether they are net-erosional,
474 net-depositional, or there is a balance between erosion and deposition over longer (100s to
475 1,000 years) periods¹⁷. Channels formed by long-term net-erosion, often termed submarine
476 canyons, may contain only thin deposits with limited preservation potential. In contrast,
477 areas of net-deposition will tend to produce systems confined by levees raised high above
478 the surrounding seafloor⁶⁵, and they will have better potential for preservation in the rock
479 record. Bute Inlet appears to represent an intermediate situation, in which erosion and
480 deposition along the submarine channel are nearly balanced. Thus, over longer time scales,
481 the knickpoint deposits in such settings will not be fully preserved as they are formed here;
482 they will be mostly reworked by successive knickpoint erosion and deposition. Only if the
483 system reaches a net-depositional stage or moves laterally, parts of these deposits might be
484 preserved.

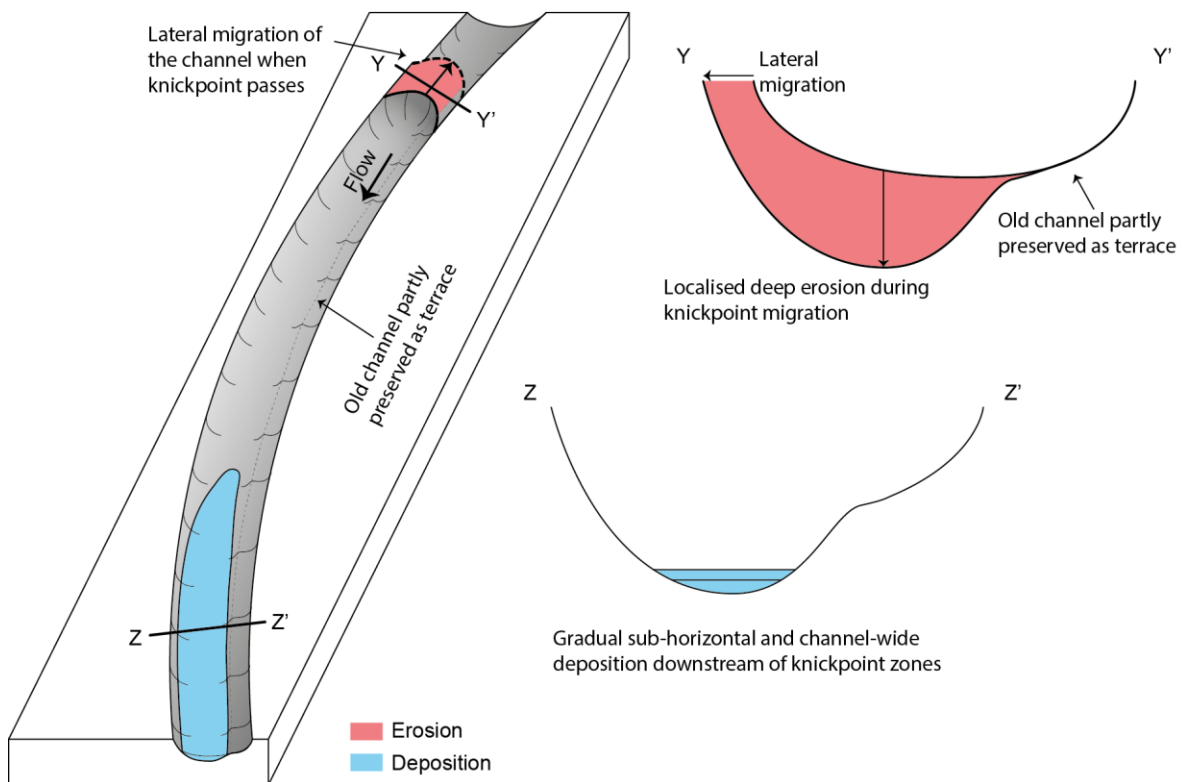
485 Similar knickpoints occur in other locations worldwide

486 Various types and dimensions of seabed knickpoints have been documented in
487 numerous locations worldwide^{22,53} (Supplementary table 2). These locations include
488 knickpoints with broadly similar dimensions that occur in active submarine and sub-
489 lacustrine ^{55,69,77} channel systems. Some of these examples are associated with steep sand-
490 rich channel fills^{24,70}. Knickpoints in other systems are often linked to tectonics, bedrock
491 outcrop or meander-bend cut-off^{22,56}. However, similar knickpoints are found in Monterey
492 Canyon, South China sea, and others, where a clear external trigger is also lacking^{24,54}. The
493 type of knickpoints seen in Bute Inlet and other locations, can occur in a wide range of

a: Meandering dominated channel deposits



b: Knickpoint dominated channel deposits



494

495 *Figure 8. Generalised models for submarine channel evolution and deposits. (a) Model of Sylvester et*

496 *al. (2011) for meandering dominated channels. This results in bars (shown in light blue) deposited in*

497 *the inner bends, and erosion in the outer bends. The erosion causes outward and downstream*

498 *propagation of bends. (b) New model for submarine channel deposits in locations dominated by fast-*

499 *moving knickpoints, such as Bute Inlet. Knickpoint migration causes deep erosion, which is then*

500 *followed by channel-wide deposition, once the knickpoint has migrated further upslope.*

501 systems, including locations with low ($<1^\circ$) gradients. Furthermore, erosional features that
502 share similarities with knickpoints have been reported to migrate up the channels in
503 Squamish Delta²⁰. This suggests that the processes that form fast-moving channel-
504 knickpoints, and their impacts on submarine channel evolution and deposits, might be of
505 widespread importance.

506 **Conclusions: new generalised model for submarine channels**

507 We used 9 years of time-lapse bathymetry from an active submarine channel in Bute
508 Inlet, British Columbia, to study how submarine channels evolve. Rapid (100-450 m/yr)
509 upstream-migration of knickpoints was the dominate process driving channel evolution.
510 Previously described processes such as meander-bend migration, levee aggradation, and
511 migration of smaller bedforms all play a minor role in channel evolution on this time scale in
512 Bute Inlet. Knickpoints are steep (up to angle of repose) steps in channel gradient, with
513 heights of up to 30 m. Sediment upstream of a knickpoint is eroded during migration and
514 deposition occurs further downstream of the knickpoint. Deposits form long and thin
515 channel-wide deposits, rather than previously proposed bend-related bars. Knickpoints can
516 migrate outside the banks of the original channel, causing lateral migration of the channel
517 and development of channel bends. Previous models proposed outer-bend erosion and
518 inner-bend deposition is the main control on channel development and the resulting
519 deposition. However, here we propose an alternative model controlled by knickpoints.
520 Finally, we show that knickpoints are common in a variety of subaqueous settings
521 worldwide, therefore implying their global importance.

522 **Methods**

523 This study uses five bathymetric surveys spanning a total of nine years, collected in
524 March 2008, November 2010, February 2015, June 2016, and October 2016. Past work has
525 considered only the first two surveys in 2008 and 2010^{62,63}. The March 2008 survey was
526 obtained using a Kongsberg-Simrad EM 1002 (100 kHz) multibeam echosounder. The later
527 surveys used a Kongsberg Maritime EM710 (70-100 kHz) multibeam echosounder,
528 controlled using Kongsberg Maritime SIS software.

529 Data were processed to correct for differences in sound velocity of the water (using
530 data from a sound velocity profiler), together with tides, waves, and ship's motion. The
531 vertical resolution of bathymetric data is ~0.5% of the water depth, and is thus a maximum
532 of ~3 metres at the channel termination at water depths of ~600 m (Supplementary Fig.
533 2b,c,d). Bathymetry was then processed to calculate the local gradient, in order to optimally
534 display small steep topographic features such as knickpoints.

535 Patterns of erosion and deposition are visualised using bathymetric difference maps,
536 calculated by subtracting two surveys from each other. These difference maps were then
537 used to estimate volumes of different erosional processes. First, the total eroded volume
538 within the active channel is calculated (Supplementary Fig. 3). Then, parts of that eroded
539 volume are attributed to either outer-bend erosion or knickpoint migration, based on the
540 geometry and location of erosional areas (Supplementary Fig. 3). Steep areas such as fjord
541 sidewalls and the overbanks have not been taken into account, because volumetric
542 calculations including these areas will reflect uncertainties rather than real change. Reliable
543 volumetric calculations and mass balances of the deposition cannot be made, as the thin

544 and widespread geometry of depositional bodies often falls below resolution of the surveys,
545 especially on the overbanks.

546 The bathymetric surveys were used to construct along-channel profiles. The position
547 of the channel shifts as the channel evolves, so profiles were constructed along the position
548 of the thalweg in that survey. The different along-channel profiles were all normalised to
549 before comparing.

550 **Data availability**

551 The data that support the findings of this study are available from the corresponding author
552 upon reasonable request.

553 **References**

- 554 1. Curray, J. R., Emmel, F. J. & Moore, D. G. The Bengal Fan: morphology, geometry,
555 stratigraphy, history and processes. *Mar. Pet. Geol.* **19**, 1191–1223 (2002).
- 556 2. Khripounoff, A. *et al.* Direct observation of intense turbidity current activity in the Zaire
557 submarine valley at 4000 m water depth. *Mar. Geol.* **194**, 151–158 (2003).
- 558 3. Talling, P. J. On the triggers, resulting flow types and frequencies of subaqueous sediment
559 density flows in different settings. *Mar. Geol.* **352**, 155–182 (2014).
- 560 4. Wynn, R. B., Cronin, B. T. & Peakall, J. Sinuous deep-water channels: Genesis, geometry and
561 architecture. *Mar. Pet. Geol.* **24**, 341–387 (2007).
- 562 5. Peakall, J. & Sumner, E. J. Submarine channel flow processes and deposits: A process-product
563 perspective. *Geomorphology* **244**, 95–120 (2015).
- 564 6. Heezen, B. C. & Ewing, M. Turbidity currents and submarine slumps, and the 1929 Grand
565 Banks Earthquake. *American Journal of Science* **250**, 849–873 (1952).
- 566 7. Carter, L. *et al.* *Submarine cables and the oceans: connecting the world.* *Journal of the*
567 *Franklin Institute* **108**, (2009).
- 568 8. Pope, E. L., Talling, P. J. & Carter, L. Which earthquakes trigger damaging submarine mass
569 movements: Insights from a global record of submarine cable breaks? *Mar. Geol.* **384**, 131–
570 146 (2017).
- 571 9. Canals, M. *et al.* Flushing submarine canyons. *Nature* **444**, 354–357 (2006).
- 572 10. Vangriesheim, A. *et al.* The influence of Congo River discharges in the surface and deep layers
573 of the Gulf of Guinea. *Deep Sea Res. Part II Top. Stud. Oceanogr.* **56**, 2183–2196 (2009).
- 574 11. Kane, I. A. & Clare, M. A. Dispersion, Accumulation, and the Ultimate Fate of Microplastics in
575 Deep-Marine Environments: A Review and Future Directions. *Front. Earth Sci.* **7**, 80 (2019).
- 576 12. Mayall, M., Jones, E. & Casey, M. Turbidite channel reservoirs—Key elements in facies
577 prediction and effective development. *Mar. Pet. Geol.* **23**, 821–841 (2006).
- 578 13. Baudin, F., Disnar, J.-R., Martinez, P. & Dennielou, B. Distribution of the organic matter in the
579 channel-levees systems of the Congo mud-rich deep-sea fan (West Africa). Implication for
580 deep offshore petroleum source rocks and global carbon cycle. *Mar. Pet. Geol.* **27**, 995–1010
581 (2010).
- 582 14. Prins, M. A. & Postma, G. Effects of climate, sea level, and tectonics unraveled for last
583 deglaciation turbidite records of the Arabian Sea. *Geology* **28**, 375 (2000).

- 584 15. Clift, P. & Gaedicke, C. Accelerated mass flux to the Arabian Sea during the middle to late
585 Miocene. *Geology* **30**, 207 (2002).
- 586 16. Talling, P. J. *et al.* Onset of submarine debris flow deposition far from original giant landslide.
587 *Nature* **450**, 541–544 (2007).
- 588 17. Covault, J. A. Submarine fans and canyon-channel systems: a review of processes, products,
589 and models. *Nat. Educ. Knowl.* **3**, 4 (2011).
- 590 18. Fildani, A. *et al.* Erosion at inception of deep-sea channels. *Mar. Pet. Geol.* **41**, 48–61 (2013).
- 591 19. Hughes Clarke, J. E. First wide-angle view of channelized turbidity currents links migrating
592 cyclic steps to flow characteristics. *Nat. Commun.* **7**, 1–13 (2016).
- 593 20. Vendettuoli, D. *et al.* Daily bathymetric surveys document how stratigraphy is built and its
594 extreme incompleteness in submarine channels. *Earth Planet. Sci. Lett.* **515**, 231–247 (2019).
- 595 21. Constantine, J. A. & Dunne, T. Meander cutoff and the controls on the production of oxbow
596 lakes. *Geology* **36**, 23 (2008).
- 597 22. Heiniö, P. & Davies, R. J. Knickpoint migration in submarine channels in response to fold
598 growth, western Niger Delta. *Mar. Pet. Geol.* **24**, 434–449 (2007).
- 599 23. de Leeuw, J., Eggenhuisen, J. T. & Cartigny, M. J. B. Morphodynamics of submarine channel
600 inception revealed by new experimental approach. *Nat. Commun.* **7**, 10886 (2016).
- 601 24. Paull, C., Caress, D. W., Ussler, W., Lundsten, E. & Meiner-Johnson, M. High-resolution
602 bathymetry of the axial channels within Monterey and Soquel submarine canyons, offshore
603 central California. *Geosphere* **7**, 1077 (2011).
- 604 25. Sylvester, Z., Pirmez, C. & Cantelli, A. A model of submarine channel-levee evolution based on
605 channel trajectories: Implications for stratigraphic architecture. *Mar. Pet. Geol.* **28**, 716–727
606 (2011).
- 607 26. Hubbard, S. M., Covault, J. A., Fildani, A. & Romans, B. W. Sediment transfer and deposition in
608 slope channels: Deciphering the record of enigmatic deep-sea processes from outcrop. *Geol.*
609 *Soc. Am. Bull.* **126**, 857–871 (2014).
- 610 27. Peakall, J., Amos, K. J., Keevil, G. M., William Bradbury, P. & Gupta, S. Flow processes and
611 sedimentation in submarine channel bends. *Mar. Pet. Geol.* **24**, 470–486 (2007).
- 612 28. Covault, J. A., Sylvester, Z., Hudec, M. R., Ceyhan, C. & Dunlap, D. Submarine channels ‘swept’
613 downstream after bend cutoff in salt basins. *Depos. Rec.* dep2.75 (2019).
614 doi:10.1002/dep2.75
- 615 29. Dietrich, W. E., Smith, J. D. & Dunne, T. Flow and Sediment Transport in a Sand Bedded
616 Meander. *J. Geol.* **87**, 305–315 (1979).
- 617 30. Parker, G. & Andrews, E. On the time development of meander bends. *J. Fluid Mech.* **162**,
618 139–156 (1986).
- 619 31. Azpiroz-Zabala, M. *et al.* A General Model for the Helical Structure of Geophysical Flows in
620 Channel Bends. *Geophys. Res. Lett.* **44**, 11,932–11,941 (2017).
- 621 32. Sylvester, Z., Durkin, P. & Covault, J. A. High curvatures drive river meandering. *Geology* **47**,
622 263–266 (2019).
- 623 33. Lewis, G. W. & Lewin, J. Alluvial Cutoffs in Wales and the Borderlands. in *Modern and Ancient*
624 *Fluvial Systems* 145–154 (Blackwell Publishing Ltd., 2009). doi:10.1002/9781444303773.ch11
- 625 34. Peakall, J., McCaffrey, B. & Kneller, B. A Process Model for the Evolution, Morphology, and
626 Architecture of Sinuous Submarine Channels. *J. Sediment. Res.* **70**, 434–448 (2000).
- 627 35. Corney, R. K. T. *et al.* The orientation of helical flow in curved channels. *Sedimentology* **53**,
628 249–257 (2006).
- 629 36. Imran, J. *et al.* Helical flow couplets in submarine gravity underflows. *Geology* **35**, 659–662
630 (2007).
- 631 37. KOLLA, V., BANDYOPADHYAY, A., GUPTA, P., MUKHERJEE, B. & V.RAMANA, D. Morphology
632 and Internal Structure of a Recent Upper Bengal Fan-Valley Complex. in *Application of the*
633 *Principles of Seismic Geomorphology to Continental-Slope and Base-of-Slope Systems: Case*
634 *Studies from Seafloor and Near-Seafloor Analogues* 347–369 (2012).

- doi:10.2110/pec.12.99.0347
- 636 38. Imran, J., Parker, G. & Katopodes, N. A numerical model of channel inception on submarine
637 fans. *J. Geophys. Res. Ocean.* **103**, 1219–1238 (1998).
- 638 39. Rowland, J. C., Hilley, G. E. & Fildani, A. A Test of Initiation of Submarine Leveed Channels by
639 Deposition Alone. *J. Sediment. Res.* **80**, 710–727 (2010).
- 640 40. Damuth, J. E., Flood, R. D., Kowsmann, R. O., Belderson, R. H. & Gorini, M. A. Anatomy and
641 growth pattern of Amazon deep-sea fan as revealed by long-range side-scan sonar (GLORIA)
642 and high-resolution seismic studies. *AAPG Bull.; (United States)* **72:8**, (1988).
- 643 41. Komar, P. D. Hydraulic Jumps in Turbidity Currents. *Geol. Soc. Am. Bull. vol. 82, issue 6, p.*
644 *1477* **82**, 1477 (1971).
- 645 42. Fildani, A., Normark, W. R., Kostic, S. & Parker, G. Channel formation by flow stripping: Large-
646 scale scour features along the Monterey East Channel and their relation to sediment waves.
647 *Sedimentology* **53**, 1265–1287 (2006).
- 648 43. Paull, C. K. *et al.* Origins of large crescent-shaped bedforms within the axial channel of
649 Monterey Canyon, Offshore California. *Geosphere* **6**, 755–774 (2010).
- 650 44. Covault, J. A., Kostic, S., Paull, C. K., Ryan, H. F. & Fildani, A. Submarine channel initiation,
651 filling and maintenance from sea-floor geomorphology and morphodynamic modelling of
652 cyclic steps. *Sedimentology* **61**, 1031–1054 (2014).
- 653 45. Covault, J. A., Kostic, S., Paull, C. K., Sylvester, Z. & Fildani, A. Cyclic steps and related
654 supercritical bedforms: Building blocks of deep-water depositional systems, western North
655 America. *Marine Geology* **393**, 4–20 (2017).
- 656 46. Hage, S. *et al.* How to recognize crescentic bedforms formed by supercritical turbidity
657 currents in the geologic record: Insights from active submarine channels. *Geology* **46**, 563–
658 566 (2018).
- 659 47. Gardner, T. W. Experimental study of knickpoint and longitudinal profile evolution in
660 cohesive, homogeneous material. *Geol. Soc. Am. Bull.* **94**, 664–572 (1983).
- 661 48. Howard, A. D., Dietrich, W. E. & Seidl, M. A. Modeling fluvial erosion on regional to
662 continental scales. *J. Geophys. Res. Solid Earth* **99**, 13971–13986 (1994).
- 663 49. van Heijst, M. W. I. M. & Postma, G. Fluvial response to sea-level changes: a quantitative
664 analogue, experimental approach. *Basin Res.* **13**, 269–292 (2001).
- 665 50. Hayakawa, Y. & Matsukura, Y. Recession rates of waterfalls in Boso Peninsula, Japan, and a
666 predictive equation. *Earth Surf. Process. Landforms* **28**, 675–684 (2003).
- 667 51. Crosby, B. T. & Whipple, K. X. Knickpoint initiation and distribution within fluvial networks:
668 236 waterfalls in the Waipaoa River, North Island, New Zealand. *Geomorphology* **82**, 16–38
669 (2006).
- 670 52. Burbank, D. W. & Anderson, R. S. (Robert S. *Tectonic geomorphology*. (J. Wiley & Sons, 2012).
- 671 53. Mitchell, N. C. Morphologies of knickpoints in submarine canyons. *Bull. Geol. Soc. Am.* **118**,
672 589–605 (2006).
- 673 54. Zhong, G., Cartigny, M. J. B., Kuang, Z. & Wang, L. Cyclic steps along the South Taiwan Shoal
674 and West Penghu submarine canyons on the northeastern continental slope of the South
675 China Sea. *Geol. Soc. Am. Bull.* **127**, 804–824 (2015).
- 676 55. Turmel, D., Locat, J. & Parker, G. Morphological evolution of a well-constrained, subaerial-
677 subaqueous source to sink system: Wabush Lake. *Sedimentology* **62**, 1636–1664 (2015).
- 678 56. Sylvester, Z. & Covault, J. A. Development of cutoff-related knickpoints during early evolution
679 of submarine channels. *Geology* **44**, 835–838 (2016).
- 680 57. Syvitski, J. P. M. & Farrow, G. E. Structures and processes in bayhead deltas: Knight and Bute
681 inlet, British Columbia. *Sediment. Geol.* **36**, 217–244 (1983).
- 682 58. Prior, D. B., Bornhold, B. D. & Johns, M. W. Active sand transport along a fjord-bottom
683 channel, Bute Inlet, British Columbia. *Geology* **14**, 581–584 (1986).
- 684 59. Prior, D. B., Bornhold, B. D., Wiseman, W. J. & Lowe, D. R. Turbidity current activity in a British
685 Columbia Fjord. *Science (80-)*. **237**, 1330–1333 (1987).

- 686 60. Zeng, J., Lowe, D. R., Prior, D. B., Wiseman, W. J. & Bornhold, B. D. Flow properties of
687 turbidity currents in Bute Inlet, British Columbia. *Sedimentology* **38**, 975–996 (1991).
- 688 61. Bornhold, B. D., Ren, P. & Prior, D. B. High-frequency turbidity currents in British Columbia
689 fjords. *Geo-Marine Lett.* **14**, 238–243 (1994).
- 690 62. Conway, K. W., Barrie, J. V., Picard, K. & Bornhold, B. D. Submarine channel evolution: Active
691 channels in fjords, British Columbia, Canada. *Geo-Marine Lett.* **32**, 301–312 (2012).
- 692 63. Gales, J. A. *et al.* What controls submarine channel development and the morphology of
693 deltas entering deep-water fjords? *Earth Surface Processes and Landforms* (2018).
694 doi:10.1002/esp.4515
- 695 64. Maier, K. L. *et al.* Punctuated Deep-Water Channel Migration: High-Resolution Subsurface
696 Data from the Lucia Chica Channel System, Offshore California, U.S.A. *J. Sediment. Res.* **82**, 1–
697 8 (2012).
- 698 65. Deptuck, M. E., Steffens, G. S., Barton, M. & Pirmez, C. Architecture and evolution of upper
699 fan channel-belts on the Niger Delta slope and in the Arabian Sea. *Mar. Pet. Geol.* **20**, 649–
700 676 (2003).
- 701 66. Hodgson, D. M., Kane, I. A., Flint, S. S., Brunt, R. L. & Ortiz-Karpf, A. Time-Transgressive
702 Confinement On the Slope and the Progradation of Basin-Floor Fans: Implications For the
703 Sequence Stratigraphy of Deep-Water Deposits. *J. Sediment. Res.* **86**, 73–86 (2016).
- 704 67. Yu, B. *et al.* Experiments on Self-Channelized Subaqueous Fans Emplaced by Turbidity
705 Currents and Dilute Mudflows. *J. Sediment. Res.* **76**, 889–902 (2006).
- 706 68. Toniolo, H. & Cantelli, A. Experiments on Upstream-Migrating Submarine Knickpoints. *J.*
707 *Sediment. Res.* **77**, 772–783 (2007).
- 708 69. Corella, J. P. *et al.* The role of mass-transport deposits and turbidites in shaping modern
709 lacustrine deepwater channels. *Mar. Pet. Geol.* **77**, 515–525 (2016).
- 710 70. Hill, P. R. Changes in Submarine Channel Morphology and Slope Sedimentation Patterns from
711 Repeat Multibeam Surveys in the Fraser River Delta, Western Canada. in *Sediments,*
712 *Morphology and Sedimentary Processes on Continental Shelves* 47–69 (John Wiley & Sons,
713 Ltd, 2012). doi:10.1002/9781118311172.ch3
- 714 71. Marín, L., Forman, S. L., Valdez, A. & Bunch, F. Twentieth century dune migration at the Great
715 Sand Dunes National Park and Preserve, Colorado, relation to drought variability.
716 *Geomorphology* **70**, 163–183 (2005).
- 717 72. Levoy, F., Anthony, E. J., Monfort, O., Robin, N. & Bretel, P. Formation and migration of
718 transverse bars along a tidal sandy coast deduced from multi-temporal Lidar datasets. *Mar.*
719 *Geol.* **342**, 39–52 (2013).
- 720 73. Lamb, M. P. *et al.* Evidence for superelevation, channel incision, and formation of cyclic steps
721 by turbidity currents in Eel Canyon, California. *Bull. Geol. Soc. Am.* **120**, 463–475 (2008).
- 722 74. Postma, G. & Cartigny, M. J. B. Supercritical and subcritical turbidity currents and their
723 deposits--A synthesis. *Geology* **42**, 987–990 (2014).
- 724 75. Paull, C. K. *et al.* Origins of large crescent-shaped bedforms within the axial channel of
725 Monterey Canyon, Offshore California. *Geosphere* **6**, 755–774 (2010).
- 726 76. Iverson, R. M. *et al.* Positive feedback and momentum growth during debris-flow
727 entrainment of wet bed sediment. *Nat. Geosci.* **4**, 116–121 (2011).
- 728 77. Turmel, D., Locat, J. & Parker, G. Upstream Migration of Knickpoints: Geotechnical
729 Considerations. in *Submarine Mass Movements and Their Consequences* 123–132 (Springer
730 Netherlands, 2012). doi:10.1007/978-94-007-2162-3_11
- 731 78. Holland, W. N. & Pickup, G. Flume study of knickpoint development in stratified sediment.
732 *Bull. Geol. Soc. Am.* **87**, 76–82 (1976).
- 733 79. Mutti, E. & Normark, W. R. Comparing Examples of Modern and Ancient Turbidite Systems:
734 Problems and Concepts. in *Marine Clastic Sedimentology* 1–38 (Springer Netherlands, 1987).
735 doi:10.1007/978-94-009-3241-8_1
- 736 80. Hickin, E. J. The development of meanders in natural river-channels. *Am. J. Sci.* **274**, 414–442

737 (1974).
738 81. Parker, G., Diplas, P. & Akiyama, J. Meander Bends of High Amplitude. *J. Hydraul. Eng.* **109**,
739 1323–1337 (1983).
740

741 **Acknowledgements**

742 This project has received funding from the European Union’s Horizon 2020 research and
743 innovation programme under the Marie Skłodowska-Curie grant agreement No 721403.
744 Clare, Cartigny, and Talling acknowledge funding from the Natural Environment Research
745 Council (NERC), including “Environmental Risks to Infrastructure: Identifying and Filling the
746 Gaps” (NE/P005780/1) and “New field-scale calibration of turbidity current impact
747 modelling” (NE/P009190/1). The authors also acknowledge discussions with collaborators as
748 part of Talling’s NERC International Opportunities Fund grant (NE/ M017540/1)
749 “Coordinating and pump-priming international efforts for direct monitoring of active
750 turbidity currents at global test sites”. Talling was supported by a NERC and Royal Society
751 Industry Fellowship hosted by the International Cable Protection Committee. We also
752 acknowledge support from the Canadian Geological Survey. We further thank the Canadian
753 Geological Survey and Canadian Hydrographic Survey for data collection and processing, in
754 particular Peter Neelands and Brent Seymour. Lastly, we thank the captains and crew of
755 CCGS *Vector*.

756 **Author Contributions**

757 Maarten S. Heijnen: First author, wrote most of the manuscript and performed
758 most of the data analysis
759 Michael A. Clare: Contributed to overall design of the project, data collection,
760 analysis, and writing of the manuscript

761 Matthieu J.B. Cartigny: Contributed to overall design of the project data collection,
762 analysis, and writing of the manuscript

763 Peter J. Talling Contributed to overall design of the project, data collection,
764 analysis, and writing of the manuscript

765 Sophie Hage Contributed to data collection, and analysis

766 D. Gwyn Lintern Contributed to design of the project, expedition planning and
767 organisation, and data collection

768 Cooper Stacey Contributed to expedition planning and organisation, and data
769 collection

770 Daniel R. Parsons Contributed to design of the project, and data collection

771 Stephen M. Simmons Contributed to data collection

772 Ye Chen Contributed to data analysis

773 Esther J. Sumner Contributed to overall design of the project, and data
774 collection

775 Justin K. Dix Contributed to writing of the manuscript

776 John E. Hughes Clarke Contributed to overall design of the project, data collection,
777 and analysis